Nanoparticle Doping for Improved Er-doped Fiber Lasers

Colin C. Baker[a], E. Joseph Friebele[a], Charles G. Askins[a], Michael P. Hunt,[a] Barbara A. Marcheschi[a], Jake Fontana[a], John R. Peele[b], Woohong Kim[a], Jasbinder Sanghera[a], Jun Zhang[c], Radha K. Pattnaik[c], Larry D. Merkle[c], Mark Dubinskii[c], Youming Chen[c], Iyad A. Dajani[d], Cody Mart[e]

[a]*Naval Research Laboratory, 4555 Overlook Ave. SW, Washington, DC 20375*

[b]*Sotera Defense Systems, 430 National Business Parkway, Annapolis Junction, MD 20701*

[c]*Army Research Laboratory, 2800 Powder Mill Road, Adelphi, MD 20783*

[d]*Air Force Research Lab, 3550 Aberdeen Ave SE, Kirtland Air Force Base, NM 87117*

[e]*College of Optical Sciences, University of Arizona, Tucson, Arizona 85721*

ABSTRACT

A nanoparticle (NP) doping technique was used for making erbium-doped fibers (EDFs) for high energy lasers. The nanoparticles were doped into the silica soot of preforms, which were drawn into fibers. The Er luminescence lifetimes of the NP-doped cores are longer than those of corresponding solution-doped silica, and substantially less Al is incorporated into the NP-doped cores. Optical-to-optical slope efficiencies of greater than 71% have been measured. Initial investigations of stimulated Brillouin scattering (SBS) have indicated that SBS suppression is achieved by NP doping, where we observed a low intrinsic Brillouin gain coefficient, of ~1× 10^{-11} m/W and the Brillouin bandwidth was increased by 2.5x compared to fused silica.

Keywords: Erbium doped fiber, nanoparticles, high energy lasers, fiber lasers

1. INTRODUCTION

High energy lasers (HELs) are being developed for directed energy systems because they offer a highly effective and affordable defense capability. For practical applications, the wavelength for HELs must be >1.4 μm to avoid retinal eye damage caused by the diffuse laser beam scatter from atmospheric aerosols, dust particles, and the target itself. HEL systems must also operate in the wavelength region where there is low atmospheric absorption due to water molecules.[1,2]

Er-doped fiber lasers are attractive candidates for HEL systems because erbium (Er^{3+}) provides an operational wavelength at >1.5 μm, which is in both the eye safer region and a window of low atmospheric. Er-doped fiber technology for telecom applications has been well-developed using conventional solution doping techniques. Here, a preform is prepared by first depositing layers of optical cladding inside a pure silica substrate tube, and then a core layer of silica is deposited at a lower temperature so that it forms a low density and high surface area silica "soot." The tube is then filled with a solution of erbium and aluminum in a solvent and the Er^{3+} and Al^{3+} ions are adsorbed onto the surface of the soot. The Al ions are added to the solution to increase the solubility of Er^{3+} and help prevent Er ion clustering. The tube then undergoes further processing into a solid glass preform from which a fiber is drawn.

In order to transition from an erbium-doped fiber for telecommunications to a high energy fiber laser, the concentration of laser active Er^{3+} ions in the preform must be greatly increased both to decrease the active fiber length and to enable clad pumping where the effective Er absorption is diluted by the ratio of the areas of the core to the pump cladding. This presents significant materials problems; in spite of the addition of Al, erbium ions tend to cluster when doped in a solution. As the neighboring ion-ion distance decreases, the probability of ion-ion interaction increases. This results in excited state energy transfer mechanisms, such as upconversion and pair-induced quenching, which greatly reduce laser efficiency. Furthermore, increased Er^{3+} concentrations need to be met with a similar increase in Al concentration. This, however, will increase the core refractive index, a result that is undesirable in many cases where the required refractive index difference between core and cladding is dictated by the need for single mode guidance.

Fiber Lasers XIII: Technology, Systems, and Applications, edited by John Ballato, Proc. of SPIE
Vol. 9728, 97280T · © 2016 SPIE · CCC code: 0277-786X/16/$18 · doi: 10.1117/12.2217905

A new method for preparing EDFs for telecom amplifiers has been demonstrated by Pastouret et al.[3] and Boivin et al.[4] using Er-doped nanoparticles. In this method the Er ions were surrounded by a cage of Al and O with the aim of reducing or eliminating the Er ion-ion excited state energy transfer that leads to cooperative upconversion and pair-induced quenching. Er-doped boehmite AlOOH nanoparticles were synthesized by the aqueous co-precipitation of Er and Al precursors in a bath of controlled temperature and pH.[3,4] The particles were subsequently allowed to grow or "ripen" until they were reported to form stable NPs with sizes ranging from 50-100 nm.[3,4] The silica soot preform was then doped in the conventional manner by soaking with the NP dispersion. Thernal treatment was required to calcine the NP-doped core and drive off solvent and OH. Finally, full conversion to α-Al_2O_3 occurred during the preform consolidation and collapse steps at temperatures up to 2000 C.[3]

The results of these studies[3,4] have established that the Er-Er ion interactions can be minimized in properly synthesized NPs where the Er ions are shielded from each other by surrounding them with a cage of Al and O ions. In addition, although the Al/Er ratio was as high as 350 in one case,[4] the net [Al] was much less than in a comparable solution-doped fiber. Thus, the laser properties of the EDF could be optimized through the NP synthesis while the waveguide properties of the fiber were independently controlled without the concomitant core index of refraction increase due to excess Al.

As mentioned above, the emphasis of these works was on EDF amplifiers for telecom applications, where the doping levels for Er^{3+} are much lower than are required for high energy lasers. Here we report our research using nanoparticle synthesis for Er-doped high power fiber lasers where we have increased the Er concentration to as high as 90 dB/m while minimizing excited state energy transfer between Er ions at high pump powers. We also report our initial investigations of the role of nanoparticle doping in reducing nonlinear effects in fiber lasers.

2. Experimental

Various concentrations of Al and Er were investigated in this research with the aim of obtaining ratios of Al/Er in the range between 10/1 and 20/1. Co-precipitation was performed by adding solutions of 0.05-0.1 mole/l $Al(NO_3)_3$ and 0.005-0.05 mole/l $ErCl_3$ dissolved in DI water together with a 5M NaOH solution to a continuously stirred water bath maintained at 100 C.[1,2] Surfactants were also used in the precursor to minimize agglomeration. A suspension immediately formed. Three ripening schedules were investigated: 95 C for 1 week; 160 C for 17 hours; and 160 for 1 week. After ripening, the suspension was centrifuged and washed 4 times in DI water and then washed twice in methanol. The nanoparticle solutions were then dispersed in methanol using probe sonication. In order to avoiding scattering of light and refractive index variations in the preform core, it is important to avoid introducing NP agglomerates into the soot, and so the NP dispersions were filtered to 0.6 μm with Millipore polypropylene pre-filters. Finally, they were doped into the preform core in a manner similar to that used for solution doping. After doping, the core was put through two drying stages in order to drive off the solvent and the surfactant, and then it was calcined at 1100 C which converts the NPs from $Er:Al(OH)_3$ or Er:AlO(OH) to alumina α-Al_2O_3:Er.

All preforms in the work were fabricated by the MCVD process; a depressed-cladding was first deposited followed by the pure silica soot core. The core was doped with the NP dispersion, and calcination under flowing oxygen was carried out as previously discussed. The core soot was subsequently consolidated, and the preform was collapsed in the standard manner. Depressed clad designs were used for NP-doped preforms of this study because we found that there was insufficient core refractive index increase from the Al in the NPs for good waveguiding. Solution-doped preforms were also made with the same Er and Al concentrations as in the nanoparticle case for comparison. Solution-doped preforms were made with matched clad designs. Preform refractive index profiles were measured with a Photon Kinetics PK-104 profiler. Spatially-resolved Er luminescence and lifetime measurements were made on polished ~0.5 mm thick preform slices using a focused spot from a 980 nm laser for excitation and measuring the luminescence with an InGaAs detector. The spatial resolution was ~25 μm. Fibers were drawn in-house on the NRL silica draw tower, and broadband spectral measurements were made with a Photon Kinetics FOA-2000 fiber measurement system. An Agilent 83437A EELED source and Ando AQ6315 OSA with 0.5 μm resolution were used to measure the Er peak absorption near 1530 nm.

Powder x-ray diffraction measurements of the dried NP dispersions were made using a Rigaku SmartLab 2kW XRD. The samples for transmission electron microscopy were prepared by placing a drop of the suspension onto a

SPI 200 mesh holey-carbon Cu TEM grid. The drop was then wicked off and the sample was allowed to dry. The TEM imagery was done using a JEOL JEM-2200FS field emission electron microscope.

Laser amplifier performance was evaluated with a master oscillator power amplifier (MOPA) test bed using a pump wavelength of 1476 nm and a signal wavelength of 1560 nm. A filter on the output was used to separate the amplified signal from the unabsorbed pump. A short length of SMF was fusion-spliced to the laser fiber for compatibility with the WDM. The starting length of laser fibers were ~20 m; the slope efficiency was measured at each length as the fiber was cut back, and the initial injected power was measured by cleaving the Er-doped laser fiber shortly after the splice with the SMF.

3. RESULTS

We have found that ripening conditions affect the nanoparticle size and morphology. In figure 1 TEM images are shown for the three ripening conditions investigated in this work. The nanoparticles ripened at 95C for 1 week form a predominantly Boehmite phase with large 50-100 nm platelets, similar to the observation of Jolivet et al. [5] Ripening for 1 week at 160 C forms longer rod shaped particles between 100-150 nm of the Bayerite phase. Finally ripening at 160 C for 17 hours has been found to form an Er-Al-oxide phase, as indicated by the corresponding XRD pattern (not shown). Each phase of nanoparticle formed was equally adept at capturing erbium ions and keeping them from clustering, and the phase is likely immaterial since it seems certain that calcination converts them all to Er-doped Al_2O_3 in any case. However the surface properties and hence level of agglomeration for each may vary. We have found that the Er-Al-oxide phase worked the best for binding the surfactant and reducing agglomeration to levels low enough for proper filtration.

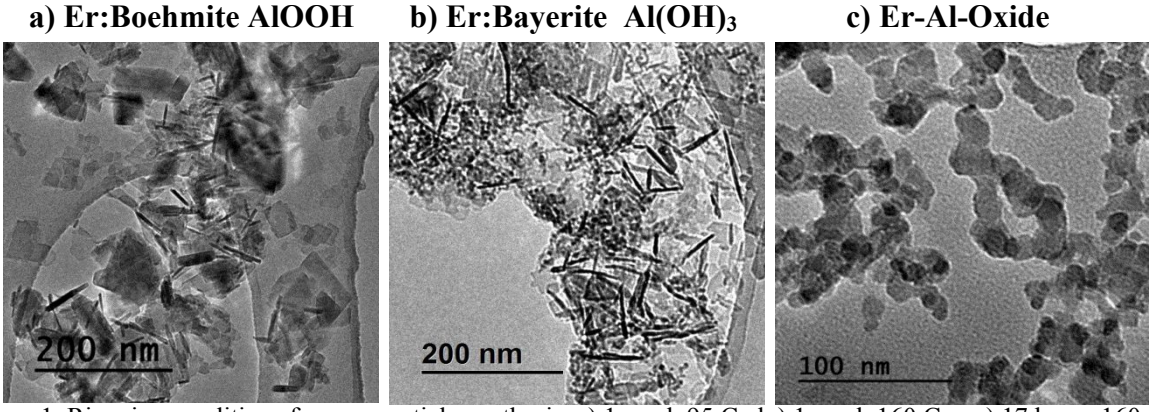

Figure 1. Ripening conditions for nanoparticle synthesis a.) 1 week 95 C b.) 1 week 160 C c.) 17 hours 160.

In comparisons of refractive index profiles for a nanoparticle-doped preform vs. solution-doped preform, figure 2, we have found that there is a much smaller refractive index increase, Δn between core and cladding for the NP case. For the NP-doped preform $\Delta n = 4x10^{-4}$, while for the solution-doped preform $\Delta n = 9x10^{-3}$, table 1. The reason for this large difference is that there is much less excess Al in NP-doped fibers because the only Al incorporated into the preform is through Al-O nanoparticles. The low value for Δn with NP addition ensures that this is an independent process parameter that can be optimized according to waveguide needs. This is important, because in a traditional solution doping method in order to add more erbium for high power, significantly more aluminum must be added. This limits the ability to tailor the waveguiding properties, since increases in aluminum cause large increases in Δn and may also result in devitrification of the SiO_2 glass. Finally, as noted earlier, large mode area fibers used in high power lasers require small values of Δn for single mode guidance.

Electron microprobe analysis of example preforms of both NP-doped and solution-doped samples indicate that the ratio of ions in the solution-doped preform is Al/Er=156, while for the NP-doped preform the ratio is Al/Er=7.4, table 1. Therefore, the NP-doped preform has 1/20 the concentration of Al ions as in the solution-doped case. It is

important to note that if a solution-doped fiber had a ratio of Al/Er of ~7, the Er emission would be highly quenched. The NP-doped preform in fact had a slightly longer luminescence lifetime, 11.0 msec, while the solution-doped preform had a lifetime of 10.8 msec, as shown in table 1.

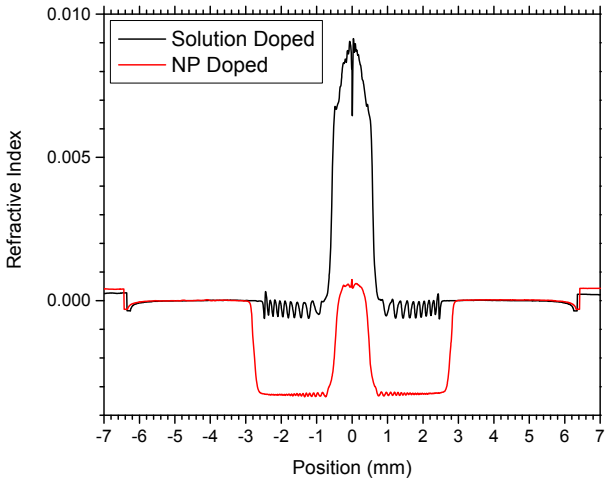

Figure 2. Refractive index profiles of preforms with NP- and solution-doped cores (Δn relative to silica)

		Electron Microprobe Analysis						
Preform	Core Δn	Al (#/m^3)	Er (#/m3)	Al/Er	Er Lifetime (ms)	Background Loss (dB/m)	Peak Abs (dB/m)	Peak Abs/Er (dB-m^2)
Solution Doped	9×10^{-3}	3.8×10^{26}	2.44×10^{24}	156	10.8	0.040	13.7	5.6×10^{24}
NP Doped	4×10^{-4}	1.48×10^{25}	2.01×10^{24}	7.4	11.0	0.039	20.0	10×10^{24}

Table 1. Optical properties of the solution-doped and NP-doped preforms and fibers and the results of electron microprobe analysis of the preform cores.

We have measured fluorescence lifetimes as long as 11.7 msec in NP-doped preforms. In figure 3 we plot fluorescence lifetime vs. intensity for more than 30 NP-doped samples and compare them to solution-doped preforms. It can be seen that there is a general trend of longer lifetimes in the NP-doped samples for the same fluorescence intensity than for solution-doped samples. These results indicate that we have reduced excited state energy transfer mechanisms that may be found in conventional solution doping techniques. This result is in accordance with the assertion that the Er^{3+} ions are effectively separated within the Al-O structure in the nanoparticles.[3]

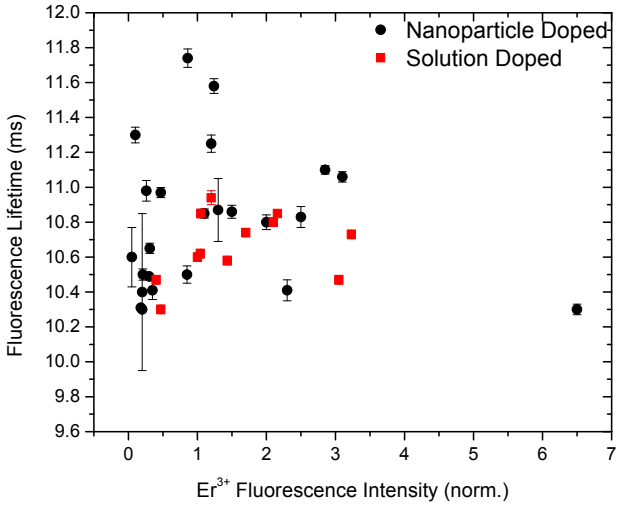

Figure 3. Fluorescence lifetime vs. intensity for NP-doped preforms and solution-doped preforms.

Erbium absorption measurements are given in figure 4. The results indicate that we are able to vary the erbium concentration in the NP-doped fibers and we have successfully obtained values for Er concentrations greater than 90 dB/m (Note that the lifetime of this sample was 11.1 msec, so this high concentration was obtained without evidence of clustering). We have also determined through cut-back spectral measurements that the background loss is very low, and in spite of the NPs being formed in an aqueous process and OH being an integral part of the NP structure, we have obtained extremely low OH group concentrations of ~0.3 ppm in the resultant fibers.

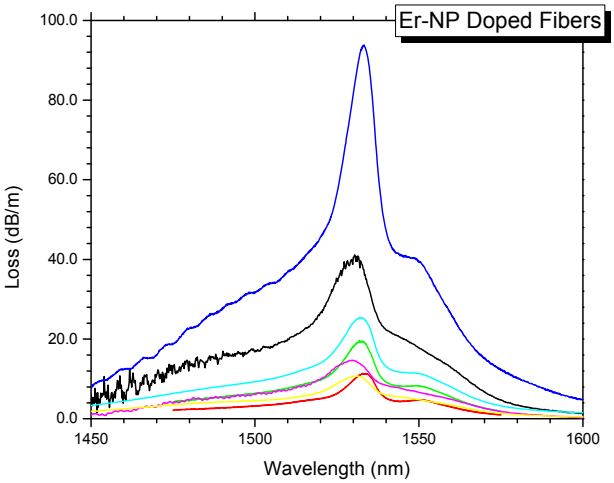

Figure 4. Erbium absorption peaks for NP-doped preforms.

MOPA results are plotted in figure 5. We have demonstrated lasing with an optical-to-optical slope efficiency of 71.5%, shown in figure 5a. The slope efficiency for several NP-doped samples is plotted as a function of Er^{3+} peak absorption in figure 5b. Values for high slope efficiency have been maintained for doping levels <40 dB/m. At higher concentrations the efficiency decreases, but the values are artificially low. These data are obtained by core pumping the fibers and collecting a signal at 1560 nm, which is an area with relatively high absorption loss. Therefore we are far from achieving gain in the fibers with high absorption. However, in a high energy laser configuration the fibers will be clad-pumped at much higher pump powers, thus achieving much more gain in the fibers, and the laser will be operating near 1600 nm in a region with lower absorption loss.

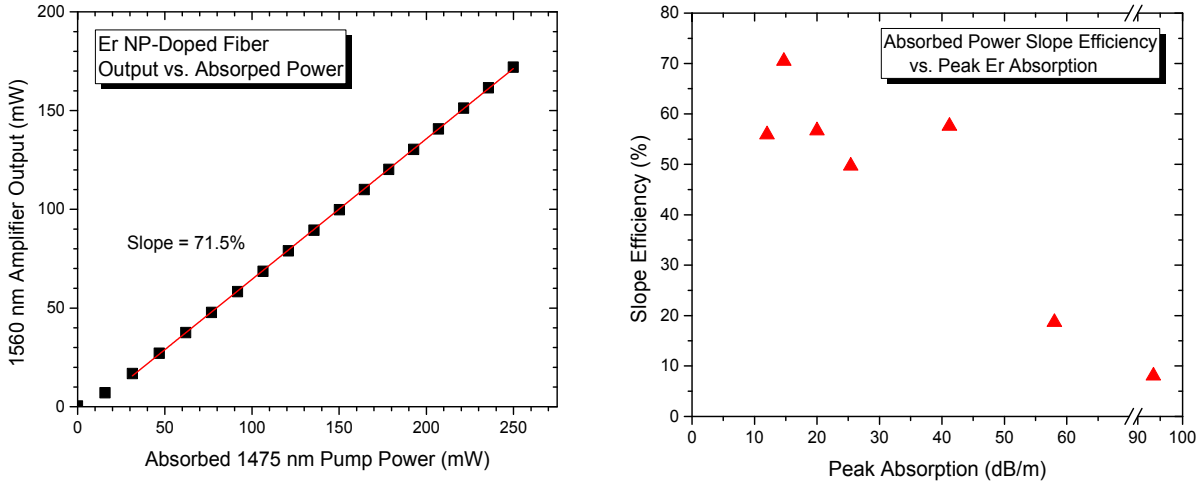

Figure 5. a.) MOPA output vs. absorbed pump power for an Er-NP-doped fiber, b.) slope efficiency for NP-doped preforms as a function of Er^{3+} absorption peak.

The principal limit to power scaling in single frequency fiber lasers is stimulated Brillouin scattering (SBS). In the SBS process, the high optical intensity in the fiber core causes the interaction of the electromagnetic wave with an acoustic wave that is initiated from thermal noise. The process is driven by electrostriction and the modulation of the refractive index in the medium due to the presence of the acoustic wave. Optical photons interacting with acoustic phonons generate frequency-downshifted photons propagating in the backward direction.[6] For pure SiO_2, the frequency shift at 1.5 μm is ~11 GHz and the spontaneous Brillouin gain bandwidth is ~20 MHz. If the SBS process reaches high levels, all incident power may be scattered in the opposite direction. Some efforts to mitigate this effect have included varying the acoustic refractive index profile in the longitudinal direction,[7] using hole assisted structures,[8] reduction of the overlap of guided optical and acoustic waves,[9] incorporation of materials of lower photoelastic coefficients than SiO_2,[10,11] and by seeding with a combination of broadband and single frequency laser beams.[12] In this work we were interested in investigating whether NP doping might offer an advantage in terms of SBS.

In our initial efforts to investigate SBS in NP-doped fibers we used pulsed 1568.15 nm excitation and an OSA to detect backscattered Rayleigh and Brillouin-shifted Stokes power. In figure 6 we compare the effects of SBS for a commercial Lucent HG980 Er-doped fiber with our NP-doped fiber. Two peaks are evident in the commercial fiber at low power, figure 6a, one peak for backscattered Rayleigh light (shorter wavelength), and a peak for the Brillouin-shifted Stokes light. At increased power there is only one peak, indicating that all the incident power has been converted to SBS in this fiber. In the nanoparticle-doped fiber, fig. 6b, at low power only the Rayleigh scattered peak is evident. At higher power the Rayleigh scattered peak is dominant and only a small amount of SBS

is evident. In comparisons of the two fibers it is evident that the SBS process is reduced in the NP-doped fiber. However, we note that the Er concentration in these fibers is somewhat different; the peak absorptions in HG980 and the NP-doped fibers are 10.3 and 25.4 dB/m, respectively, and the Al contents are unknown. We will compare the SBS from NP- and solution-doped fibers fabricated under otherwise identical conditions with identical Er concentrations, and we will obtain electron microprobe analysis of the fibers' cores to determine Er and Al contents.

In order to quantify the SBS effects shown in figure 6, a pump-probe experiment was conducted at 1064 nm. Two non-planar ring oscillators (NPRO) with nominal linewidths on the order of KHz were used in the setup as the pump and probe (Stokes) laser sources. Further amplification of these sources was achieved through the utilization of two amplifiers from IPG. Frequency tuning of the probe NPRO was accomplished by slowly modulating the temperature of the Nd:YAG crystal. The measured Brillouin gain spectrum (BGS) is shown in Fig. 7. We observed a positive Brillouin shift vs. silica due to the alumina in the NPs which caused a higher acoustic velocity in the fiber core. At 16.6 GHz, this shift is ~300 MHz greater than that for fused silica at 1064 nm. The measured spontaneous Brillouin gain bandwidth was ~100 MHz; a 2.5x increase over that of fused silica at this wavelength. We estimated the Brillouin gain coefficient to be 1×10^{-11} m/W. This is a significant decrease from ~2.5×10^{-11} m/W which is typical for a commercially available Yb-doped fiber.

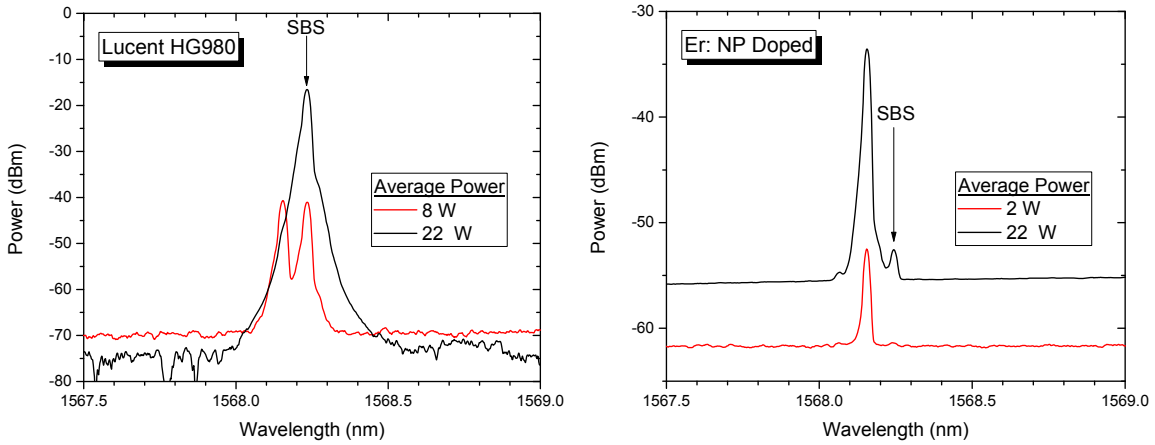

Figure 6. Backscattered Rayleigh and SBS peaks for a commercial fiber a.) and for NP-doped fiber b.)

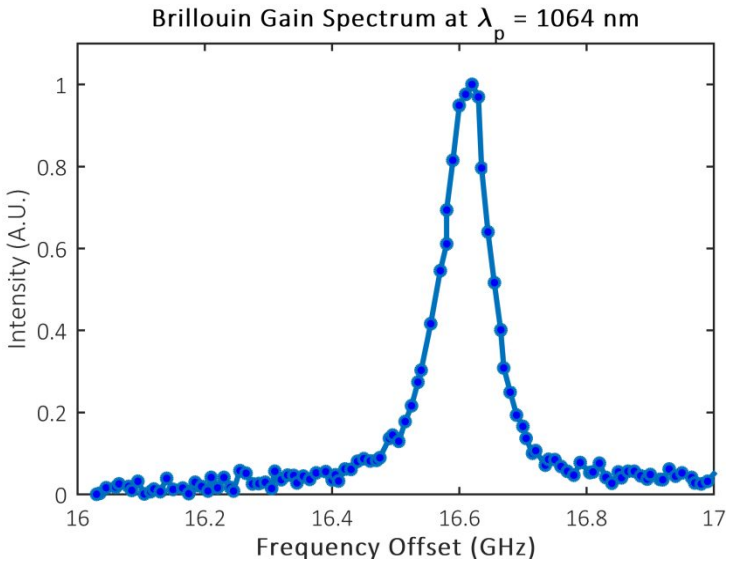

Figure 7. Brillouin gain spectrum for NP-doped fiber obtained from pump-probe experiment performed at 1064 nm

4. CONCLUSIONS

Nanoparticle doping offers an attractive method for minimizing excited state energy transfer processes in Er-doped fibers. We have synthesized nanoparticles where the Er^{3+} ions are surrounded by a cage of Al-O ions and doped them into preforms from which we have drawn high quality fibers with low background loss. We have achieved high Er concentration and low aluminum content, resulting in a greater ability to obtain low Δn required for waveguiding in large mode area fibers. Increased fluorescence lifetimes were achieved for the NP-doped fibers, indicating that excited state energy transfer processes have been reduced. We have achieved high slope efficiency with resonant pumping for relatively high doping levels. Finally, initial investigations into stimulated Brillouin scattering effects for NP-doped fibers have indicated that the SBS threshold has been increased, where the Brillouin gain coefficient is lowered and the bandwidth is increased.

REFERENCES

[1] E. J. Friebele, C. G. Askins, B. A. Marcheschi, C. C. Baker, W. Kim, J. R. Peele, J. Zhang, R. K. Pattnaik, L. D. Merkle, M. Dubinskii, "Nanoparticle doping for improved power scaling of resonantly-pumped, Yb-free Er-doped fiber lasers" in SPIE Defense, Security and Sensing Conference, Paper 9081-7 (2014).

[2] E. J. Friebele, C. C. Baker, C. G. Askins, J. P. Fontana, M. P. Hunt, J. R. Peele, B. A. Marcheschi, E. Oh, W. Kim, J. Sanghera, J. Zhang, R. K. Pattnaik, L. D. Merkle, M. Dubinskii, **"**Erbium nanoparticle-doped fibers for efficient, resonantly-pumped Er-doped fiber lasers**"** in Proc. of SPIE Vol. 9344, 934412 (2015).

[3] A. Pastouret, C. Gonnet, C. Collet, O. Cavani, E. Burov, C. Chanéac, A. Carton, and J. –P. Jolivet, "Nanoparticle doping process for improved fibre amplifiers and lasers," Proc. SPIE 7195 71951X-1-8 (2009).

[4] D. Boivin, A. Pastouret, E. Burov, C. Gonnet, O. Cavani, S. Lempereur, and P. Sillard, "Performance characterization of new erbium-doped fibers using MCVD nanoparticle doping process," Proc. SPIE 7914 , 791423-1-11 (2011).

[5] J. P. Jolivet, C. Froidefond, A. Pottier, C. Cheneac, S. Cassaignon, E. Tronc, and P. Euzen, "Size tailoring of oxide nanoparticles by precipitation in aqueous medium. A semi-quantitative modelling", J. Mater. Chem, 14 3281-3288 (2004).

[6] G. P. Agrawal*, Nonlinear Fiber Optics*, 4th ed. San Diego, CA: Academic, 329–367 (2006).

[7] K. Shiraki, M. Ohashi, and M. Tateda, "Performance of strain-free stimulated Brillouin scattering suppression fiber," J. Lightwave Technol., 14 549-554 (1996).

[8] T. Sakamoto, T. Matsui, K. Shiraki and T. Kurashima, "SBS Suppressed fiber with hole-assisted structure," J. Lightwave Technol., 27 4401-4406 (2009).
[9] M.-Jun Li, X. Chen, J. Wang, S. Gray, A. Liu, J. A. Demeritt, A. B. Ruffin, A. M. Crowley, D. T. Walton, and L. A. Zenteno, "Al/Ge co-doped large mode area fiber with high SBS threshold," Optics Express 15 8290-8299 (2007).
[10] P. D. Dragic, J. Ballato, and T. Hawkins, "Compositional tuning of glass for the suppression of nonlinear and parasitic fiber laser phenomena," Proc. of SPIE Vol. 9081 908109-2 (2014).
[11] P. D. Dragic, J. Ballato, S. Morris, and T. Hawkins, "The Brillouin gain coefficient of Yb-doped aluminosilicate glass optical fibers," Optical Materials 35 1627–1632 (2013).
[12] I. Dajani, C. Zeringue, C. Lu, C. Vergien, L. Henry, and C. Robin, "Stimulated Brillouin scattering suppression through laser gaincompetition: scalability to high power," Optics Lett. 35 3114-3116 (2010).